Silicon electrodeposition from chloride–fluoride melts containing K₂SiF₆ and SiO₂

SERGEY I. ZHUK, VLADIMIR A. ISAEV, OLGA V. GRISHENKOVA,
ANDREY V. ISAKOV*, ALEXEY P. APISAROV and YURII P. ZAYKOV

Institute of High Temperature Electrochemistry, Ural Branch of the Russian Academy of Sciences, S. Kovalevskaya St., 22, 620990, Ekaterinburg, Russian Federation

Abstract: Silicon electrodeposition on glassy carbon from KF–KCl–K₂SiF₆, KF–KCl–K₂SiF₆–KOH and KF–KCl–K₂SiF₆–SiO₂ melts was studied by cyclic voltammetry. The electroreduction of Si(IV) to metallic Si was observed as a single 4-electron wave under all the considered conditions. The reactions of cathode reduction of silicon from fluoride and oxyfluoride complexes were suggested. It was shown that the process could be controlled by the preliminary transformation of SiO_4^{4-} to SiF_6^{2-} and $SiO_xF_y^{z-}$. The influence of the current density on the structure and morphology of silicon deposits obtained during galvanostatic electrolysis of the KF–KCl–K₂SiF₆–SiO₂ melt was studied.

Keywords: silicon; electrocrystallization; molten salts; cyclic voltammetry.

INTRODUCTION

Development of renewable technologies for power generation is directly connected with the achievements in the field of the manufacture of new constructive and functional silicon materials. Electrodeposition from molten salts is a prospective method for the production of high-purity silicon and silicon-based nanomaterials.[1–5] The advantages of the electrochemical method are the possibility to control the structure and properties of deposits,[4–8] relatively simple equipment and low energy consumption.

The effective control of the electrocrystallization process requires a detailed study of many aspects, including those related to the regularities of nucleation//growth stage on an indifferent cathode,[9,10] the influence of the electrodeposition conditions (melt composition, substrate material and structure, temperature, *etc.*) on the process mechanism and kinetics, and the structure and morphology of cathode deposits.

Electrolytes based on fluorides and chlorides of alkali metals are usually used for silicon electrodeposition.[6–8,10–20] The KF–KCl–K_2SiF_6 is one of the most prospective electrolytes, as it has sufficient thermal stability, it is less aggressive than a purely fluoride one, and it is water soluble, which facilitates separation of the salt and silicon phases of the cathode deposit.[7,8,18,19] The mechanism of silicon electroreduction in this melt was studied previously.[10,18–20] It was found that during silicon electrodeposition from a KF–KCl (2:1)–0.2 mol K_2SiF_6 melt on a glassy carbon at 1023 K[10] and from KF–KCl (45:55 mole ratio)–(0.5–5 mol %) K_2SiF_6 on silver at 923 K,[18,19] a single stage Si(IV) discharge with the simultaneous transfer of 4 electrons occurred. However, another paper[20] reported a complex mechanism with the formation of intermediate silicon compounds during deposition from (KF–KCl)$_{eutectic}$–0.4 mol % K_2SiF_6 on silver at 933 K.

Silicon electrodeposition from a KF–KCl–K_2SiF_6–SiO_2 melt requires further study. There are a few works devoted to the study of the physico–chemical properties of this melt[21] and the interaction between SiO_2 and KF–KCl–K_2SiF_6.[22] Silicon deposits on graphite were obtained during the electrolysis of a KF–KCl–K_2SiF_6–SiO_2 melt.[23,24] It was shown that deposits with a high specific surface were formed when silicon dioxide was present in the melt. A more detailed study of the electrocrystallization silicon from the KF–KCl–K_2SiF_6–SiO_2 melt is of great interest both for defining the influence of oxygen-containing additions on the mechanism of the cathode process and for evaluating the possibility of performing the process in air and using more accessible raw materials (SiO_2).

The purpose of the present work was to define the influence of oxygen-containing additions (SiO_2, KOH) on the mechanism of silicon electroreduction from the KF–KCl–K_2SiF_6-based melts and the impact of the current density on structure and morphology of the silicon deposits obtained during electrodeposition from a KF–KCl–K_2SiF_6–SiO_2 melt under galvanostatic conditions.

EXPERIMENTAL

The background electrolyte was prepared from chemically pure potassium fluoride and chloride (in a mole ratio of 2:1). The mixture was melted and maintained at 973 K for 1 h, before the required amount of potassium hexafluorosilicate and, if required silicon dioxide or potassium hydroxide, were added. The procedure of the preliminary salt preparation was previously described.[21,22]

The study of the silicon electroreduction process in KF–KCl–K_2SiF_6, KF–KCl–K_2SiF_6–KOH and KF–KCl–K_2SiF_6–SiO_2 melts was performed by cyclic voltammetry in a three-electrode cell made of heat-resistant stainless steel (Fig. 1). The cell walls (1) were protected by nickel screens (2). A glassy carbon crucible (3) was placed on the graphite support (17), which was equipped with a holder (5). Tungsten rods (6, 8 and 14) served as current leads to the electrodes. A glassy carbon plate (1.5–2 cm^2) was used as the working electrode (15). Silicon monocrystalline plates (99.9999 wt. % Si) served as the auxiliary electrode (4) and

reference electrode (16). An extra pure argon atmosphere (99.998 wt. % Ar) above the melt was enabled *via* gas channels (9 and 12)*.
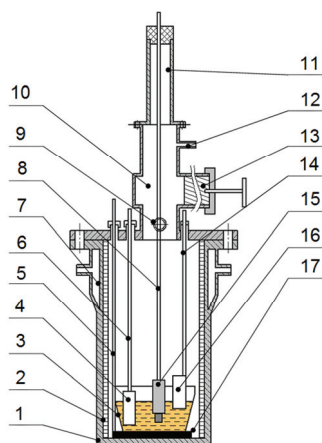

Fig. 1. Scheme of the cell for the Si electroreduction studies: 1 – heat–resistant steel cell; 2 – protection nickel screens; 3 – glassy carbon crucible; 4 – auxiliary electrode; 5 – holder; 6 – working electrode current lead; 7 – water--cooled case; 8 – working electrode current lead; 9 – gas channel; 10 – sluice chamber; 11 – cup of the sluice chamber; 12 – gas channel; 13 – sluice device; 14 – reference electrode current lead; 15 – working electrode; 16 – reference electrode; 17 – graphite support.

The prepared electrolyte was placed into the glassy carbon crucible (3), heated in vacuum to 573 K and maintained at this temperature for 3 h. Then the cell was filled with argon, the temperature increased and a stepwise potentiostatic purifying electrolysis was performed on the graphite electrode to remove all admixtures and traces of moisture in the electrolyte. Subsequently, the graphite electrode was removed from the cell *via* the sluice device (13) and the glassy carbon working electrode was inserted (15).

The cyclic voltammograms were recorded by an Autolab PGStat 302N potentiostat/galvanostat with Nova 1.5 software. Before measuring, the electrodes were kept for 30 min in the melt to set the potential. The initial values of the electrode potential were controlled before each series of measurements (the difference did not exceed 5 mV). The resistance of the measuring circuit was detected by the impedance method and compensated instrumentally. The temperature of the melt was controlled by a Pt–Pt/Rh thermocouple with an accuracy of ±1 °C.

The silicon deposits were obtained during electrolysis of the KF–KCl (2:1)–(10 mol %) K_2SiF_6–(2–3 mol %) SiO_2 melt under galvanostatic conditions. The experimental technique was described in detail previously.[23] The obtained deposits were separated from the electrode using a puller made of instrumental steel, ground, washed with an aqueous HCl (1.0 mol L^{-1}) solution at 353 K until complete removal of the electrolyte and then dried in a Pro-Analytical centrifuge at a rotation speed to 6000 rpm (Centurion Scientific Ltd., UK).

The contents of the admixtures in the melt (before and after the experiment) and in the deposits were detected by inductively coupled plasma atomic emission spectroscopy using an iCAP 6300 Duo instrument (Thermo Scientific, USA). A Sorbi N.4.1 (Meta, RF) was used to determine the specific surface of the powders. X-Ray spectral microanalysis (EDS) and SEM imaging of the samples were performed using a JMS-5900LV scanning electron microscope (Jeol, Japan). XRD analysis of the silicon powders with recognition of the crystallite sizes was realized by means of Rigaku D/MAX 2200VL/PC defractometer (Rigaku, Japan).

RESULTS AND DISCUSSION

Study of the silicon electroreduction mechanism

Typical cyclic voltammograms obtained during silicon electroreduction from a KF–KCl–K$_2$SiF$_6$ melt are presented in Fig. 2. All *i–E* dependencies demonstrated only one cathode peak, which was related to diffusion to the deposited silicon, and a corresponding anode peak of silicon dissolution. Such a shape of the curves is typical for a single stage Si(IV) discharge. Increasing the temperature (Fig. 2A) expectedly led to a growth of the cathode peak, i_p, which shifted to the region of the less negative potentials due to mass transfer acceleration. Increasing the silicon concentration in the melt (Fig. 2B) caused a proportional increase in i_p, which enabled the cathode peaks to be associated with the process of silicon electrodeposition.
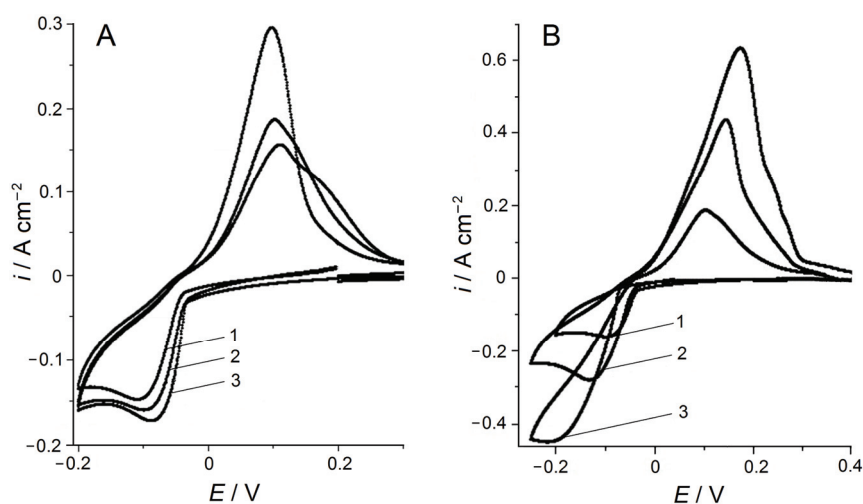

Fig. 2. Cyclic voltammograms for Si electrodeposition on glassy carbon from a KF–KCl (2:1)–K$_2$SiF$_6$ melt. Scan rate: 0.1 V s^{-1}. A) $c_{K_2SiF_6}$ = 6.65×10^{-5} mol cm^{-3}, T / K: 998 (1), 1023 (2), 1048 (3) and B) T = 1023 K, $c_{K_2SiF_6}$ / mol cm^{-3}: 6.65×10^{-5} (1); 1.13×10^{-4} (2); 1.86×10^{-4} (3).

The cyclic voltammograms recorded at different scan rates, *v*, are illustrated in Fig. 3. The i_p dependence on $v^{1/2}$, which was obtained over a wide range of scan rates (from 0.01 to 1 V s^{-1}), was not linear. Such behavior may be observed in systems with low standard rate constant of the electrode process.[25] Then, at a relatively low scan rates, the process may be controlled by diffusion. Previously, it was shown that at low Si ions concentration in the melt and *v* < 0.1 V s^{-1}, the process was controlled by diffusion.[10] Under diffusion control conditions, some authors[12,13] used the Berzins–Delahey[26] Equation to calculate the diffusion coefficient of the deposited ions, and the Mamantov Equation[27] to detect the number

of electrons. However, these equations are based on the assumption that a layer of the new phase was initially present on the electrode.[26,27] This condition did not exist in the present case as the processes of silicon crystals nucleation and growth occurs on the surface of the indifferent electrode after application of the potential.[10] The initial stages of the electrocrystallization (nucleation/growth processes) may influence significantly the value and current peak location and for this reason, the experimental curves were not analyzed quantitatively using the Berzins–Delahey and Mamantov Equations.
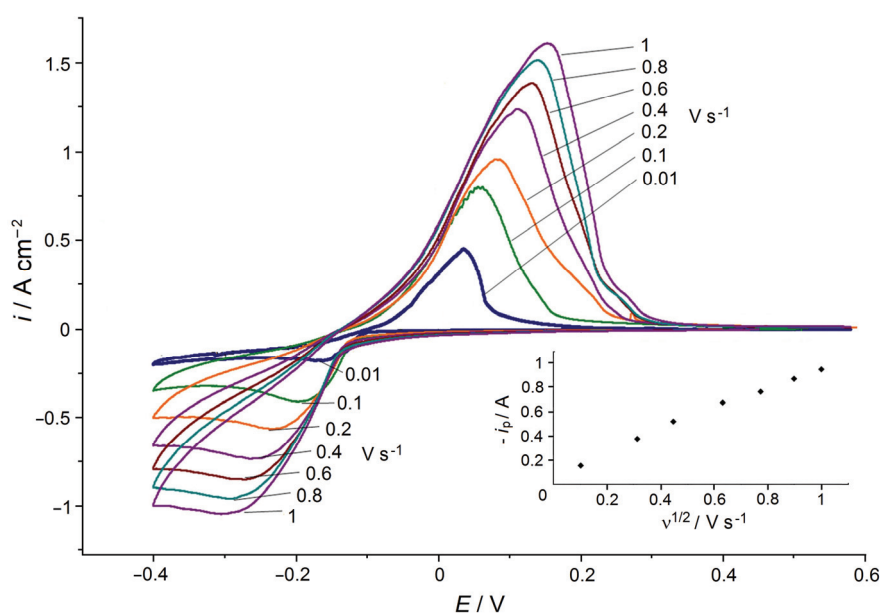
Fig. 3. Cyclic voltammograms for Si electrodeposition on glassy carbon from a KF–KCl (2:1)–K_2SiF_6 melt at 1023 K. $c_{K_2SiF_6} = 1.66\times10^{-4}$ mol cm^{-3}. Inset: the dependence of the current peak on the square root of the scan rate.

The *in situ* Raman spectroscopy[22] in the KF–KCl–K_2SiF_6 melt revealed that silicon is stable in the Si^{4+} state. Therefore, the cathode process in this case may be presented as follows:

$$SiF_6^{2-} + 4e = Si + 6F^-$$ (1)

The cyclic voltammograms obtained during silicon electrodeposition from a KF–KCl–K_2SiF_6–SiO_2 melt are shown in Fig. 4. The i_p increase corresponded to the increase in the silicon concentration in the melt containing $3.11\cdot10^{-5}$ mol cm^{-3} of SiO_2. However, a larger addition of silicon dioxide (curve 3, Fig. 4) did not result in a proportional increase of the signal. Moreover, in both cases, the common shape of the curve did not change.

A previous paper[22] reported that during the interaction of silicon dioxide with a fluoride–chloride melt, fluoride, oxyfluoride and silicate silicon complexes are formed. In a $KF–KCl–K_2SiF_6$ melt saturated with silica, the dissolution process was decelerated and a noticeable number of oxyfluoride and fluoride silicon complexes appeared only after the melt was sustained for 100 min.[22]
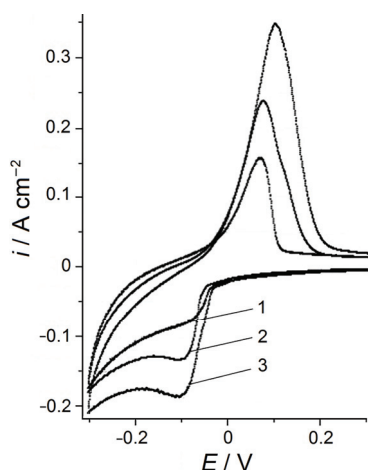

Fig. 4. Cyclic voltammograms for Si electrodeposition on glassy carbon from a $KF–KCl$ (2:1)–K_2SiF_6–SiO_2 melt at 1023 K. $c_{K_2SiF_6} = 6.65 \times 10^{-5}$ mol·cm^{-3}. c_{SiO_2}, mol·cm^{-3}: 0 (1); 3.11×10^{-5} (2) and 3.11×10^{-4} (3). Scan rate 0.1 V s^{-1}.

Thus, it may be assumed that when the large amount of SiO_2 (curve 3, Fig. 4) was added, some of the silicon ions belonging to the SiO_4^{4-} groups did not participate in the electrode process. To prove this hypothesis, an extra test to define the effect of the SiO_2 exposure time in the melt on the value of the current peak was performed. The experimental results (Fig. 5) showed that increasing the exposure time progressively increased the current peak. This data is in a good agreement with the conclusions reached in a previous study.[22]
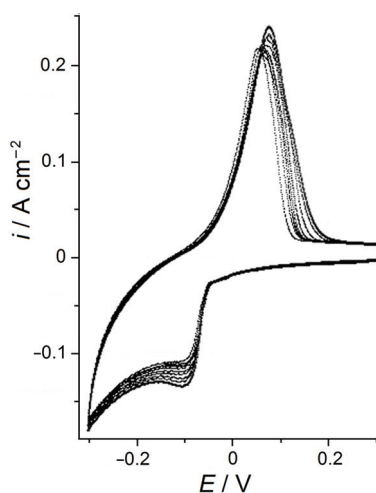

Fig. 5. Influence of the SiO_2 exposure time in the melt on the current peak. $c_{K_2SiF_6} = 6.65 \times 10^{-5}$ mol·cm^{-3}, $c_{SiO_2} = 3.11 \times 10^{-5}$ mol cm^{-3}, $T = 1023$ K. Scan rate: 0.1 V·s^{-1}. Exposure time: 60, 80, 100, 120, 150 and 180 min. The peak current increases with exposure time.

During electrodeposition from a KF–KCl–K_2SiF_6–SiO_2 melt, the shape of the cyclic voltammograms was affected by both increasing silicon concentration and the addition of oxygen-containing ions. To evaluate the impact of the later factor, silicon electrodeposition from a KF–KCl–K_2SiF_6–KOH melt was performed. It could be seen from Fig. 6 that the addition of 2.2 mol % KOH had no significant influence on the shape of the cathode part of the *i*–*E* curve. However, current peaks in the potassium hydroxide-containing melt were noticeably smaller than those in KF–KCl–K_2SiF_6 under otherwise identical conditions. Probably, this was due to the appearance of SiO_4^{4-} in the melt, according to the reaction:
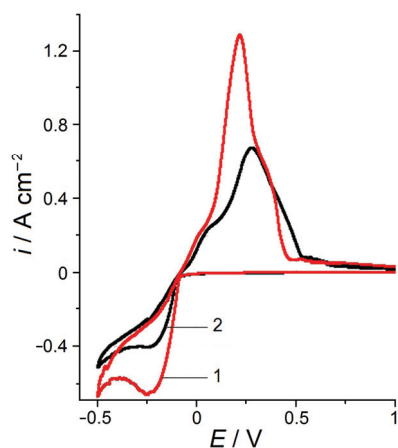
$$K_2SiF_6 + 4KOH = 2KF + K_4SiO_4 + 4HF\uparrow \tag{2}$$

Fig. 6. Cyclic voltammograms for Si electrodeposition on glassy carbon at 1023 K. The melt composition: KF–KCl (2:1)–(6.65×10^{-5} mol cm^{-3}) K_2SiF_6 (1) and KF–KCl (2:1)–(6.65×10^{-5} mol cm^{-3}) K_2SiF_6––(6.54×10^{-4} mol cm^{-3}) KOH (2). Scan rate: 0.5 $V\cdot s^{-1}$.

According to the literature,[22] the interaction between SiO_4^{4-} and F^- should lead to Si–O bond breakage and the formation of Si–F bonds, *i.e.*, to the formation of oxyfluoride and fluoride silicon groups. To prove this mechanism, the influence of the exposure time of potassium hydroxide in the melt on the cyclic voltammograms was studied (Fig. 7). As expected, the increase in exposure time resulted in an increase in the current peak.

Therefore, in KF–KCl–K_2SiF_6–KOH and KF–KCl–K_2SiF_6–SiO_2, the cathode reduction of silicon was preceded by the chemical transformation of SiO_4^{4-} into oxyfluoride and fluoride complexes. If the K_2SiF_6 concentration was low when compared to the concentration of the oxygen-containing component, the following process scheme may be suggest:
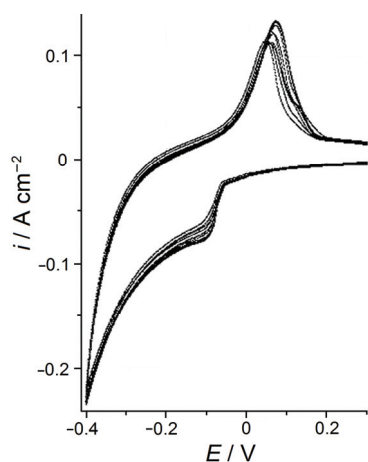
$$SiO_4^{4-} \rightarrow SiO_xF_y^{z-} + 4e = Si + xO^{2-} + yF^- \tag{3}$$
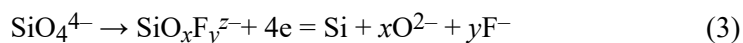
Fig. 7. Influence of the KOH exposure time in the melt on the current peak. $c_{K_2SiF_6} = 6.65 \times 10^{-5}$ mol·cm^{-3}, $c_{KOH} = 6.54 \times 10^{-4}$ mol cm^{-3} and $T = 1023$ K. Scan rate: 0.1 V·s^{-1}. Exposure time: 40, 50, 60, 80, 100, 120, 150 and 180 min. The peak current increases with exposure time.

Silicon electrodeposition

Silicon deposits were obtained during electrolysis of a KF–KCl (2:1)–10 mol % K_2SiF_6–(2–3 mol %) SiO_2 melt under galvanostatic conditions (0.02–1.5 A cm^{-2}) at 1023 K. A silicon-salt "pear" formed on the cathode; cleaned from the electrolyte, the powder-like deposit had a color from dark yellow to light brown. XRD analysis showed that the deposits were a homogeneous silicon phase. A typical diffraction pattern is shown in Fig. 8.
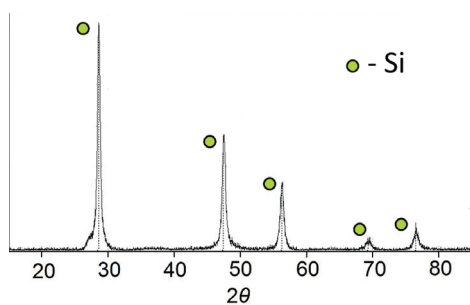

Fig. 8. Typical XRD pattern of the Si deposits obtained by electrolysis of a KF–KCl––K_2SiF_6–SiO_2 melt at 1023 K.

The SEM images of the deposits obtained at different current densities are presented in Figs. 9 and 10. Silicon was found to crystallize into fibers with an average diameter of 150–200 nm at current densities below 0.1 A cm^{-2} (Fig. 9). The formation of fiber and spongy–fibrous deposits was observed at current densities of 0.1–0.25 A cm^{-2} (Fig. 10A and B) and at higher current densities, the fiber structures degenerated (Fig. 10C and D).

The data such as those presented in Fig. 9B, allowed the suggestion that the silicon fibers are polycrystalline. The sizes of metal and semiconductor grains in
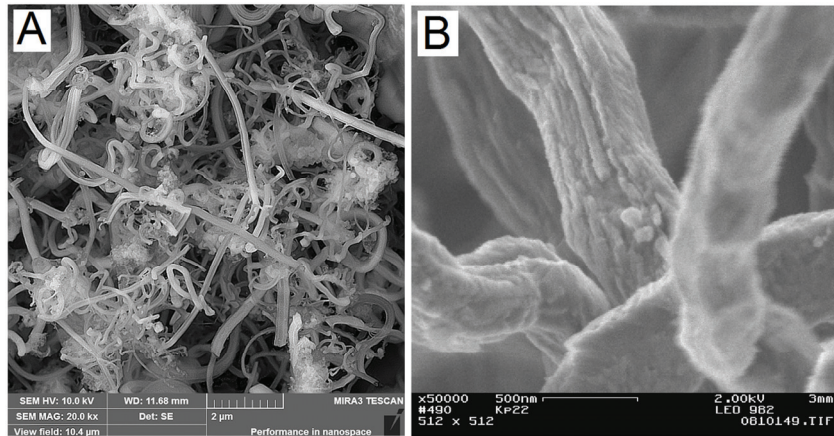
Fig. 9. SEM images of Si nanofibers obtained by electrolysis of a KF–KCl–K$_2$SiF$_6$–SiO$_2$ melt at a current density of 0.02 A·cm^{-2}, and T = 1023 K. Overall view of the deposit (A) and separate nanofibers (B).
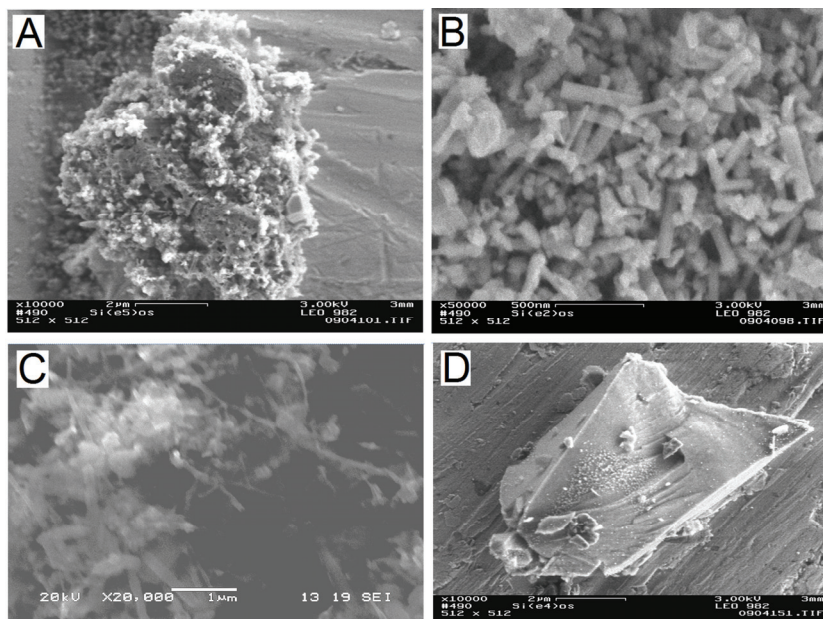

Fig. 10. SEM images of the silicon nanofiber obtained by electrolysis of a KF–KCl–K$_2$SiF$_6$–SiO$_2$ melt at 1023 K and at current densities, A·cm^{-2}: 0.1 (A); 0.25 (B); 1 (C); 0.25 (D).

the 10–200 nm range can be accurately detected by the X-ray crystallography method. The deposit characteristics obtained by X-ray crystallographic analysis are presented in Table I. The calculated values of the densities of the deposits corresponded to those for elementary silicon, within the error of the method. The

lattice parameter of deposits obtained at current densities less than 0.1 A·cm^{-2}, corresponded to the reference value. For deposits obtained at higher current densities, the lattice parameter and the elementary cell volume slightly increased, which was probably due to character changes of the electrode process (at cathode current densities higher than 0.1 A·cm^{-2}, silicon and potassium co-deposition occurs).[22,23] The data regarding the specific surface of the deposits totally agreed with the electron microscopy data. The deposits obtained at low current densities had a higher specific surface.

TABLE I. Characteristics of the silicon deposits obtained at different current densities

Current density, A·cm^{-2}	Lattice parameter. Å	Elementary cell volume, Å^3	Powder density g·cm^{-3}	Grain size nm	Specific surface m^2·g^{-1}
0.1	5.4304±0.0007	160.13	2.33	28.1±2.9	11.52
0.25	5.4413±0.0018	161.11	2.32	50.2±5.2	17.97
1.0	5.4368±0.0012	160.71	2.32	34.8±3.7	9.1
1.5	5.4338±0.0004	160.44	2.32	7.3±1.0	1.5

CONCLUSIONS

The influence of oxygen-containing additions on the mechanism of silicon electroreduction on glassy carbon during electrodeposition from KF–KCl––K$_2$SiF$_6$ based melts was studied by cyclic voltammetry. The electroreduction of Si(IV) to metallic Si was observed as a single 4-electron wave under all considered conditions. However, at silicon electrodeposition from KF–KCl–K$_2$SiF$_6$––SiO$_2$ and KF–KCl–K$_2$SiF$_6$–KOH melts, both fluoride (SiF$_6^{2-}$) and oxyfluoride (SiO$_x$F$_y^{z-}$) complexes may reduce on the cathode. Moreover, the process may be limited by preliminary SiO$_4^{4-}$ transformation into SiF$_6^{2-}$ and SiO$_x$F$_y^{z-}$.

Silicon deposits were obtained by electrolysis of a KF–KCl (2:1)–10 mol % K$_2$SiF$_6$–(2–3 mol %) SiO$_2$ melt under galvanostatic conditions at 1023 K. It was found that polycrystalline silicon nanofibers form at low cathode current densities (0.02–0.1 A cm^{-2}). Increasing the current density resulted in the formation of spongy–fibrous and powder deposits, and the grain size decreased. The deposits obtained at current densities up to 0.1 A cm^{-2} had the highest specific surface.

И З В О Д
ЕЛЕКТРОХЕМИЈСКО ТАЛОЖЕЊЕ СИЛИЦИЈУМА ИЗ ХЛОРИДНО–ФЛУОРИДНИХ
РАСТОПА K$_2$SIF$_6$ И SIO$_2$

SERGEY I. ZHUK, VLADIMIR A. ISAEV, OLGA V. GRISHENKOVA, ANDREY V. ISAKOV*, ALEXEY P. APISAROV
и YURII P. ZAYKOV

Institute of High Temperature Electrochemistry, Ural Branch of Russian Academy of Sciences, S. Kovalevskaya St., 22, 620990, Ekaterinburg, Russian Federation

Електрохемијско таложење силицијума на стакластом угљенику из растопа KF–KCl–K$_2$SiF$_6$, KF–KCl–K$_2$SiF$_6$–KOH и KF–KCl–K$_2$SiF$_6$–SiO$_2$ испитивано је цикличном

волтаметријом. Показано је да се под свим разматраним условима електрохемијска редукција јона Si(IV) до металног Si одиграва кроз један волтаметријски максимум. У раду су предложени ступњеви у редукцији силицијума из флуоридних и оксофлуоридних комплекса. Показано је да процес може бити контролисан претходном трансформацијом SiO_4^{4-} до SiF_6^{2-} и $SiO_xF_y^{z-}$. Такође је испитиван утицај густине струје на морфологију исталоженог силицијума током галваностатског таложења из растопа KF–KCl––K_2SiF_6–SiO_2.

REFERENCES

1. E. Olsen, S. Rolseth, *Met. Mat. Trans., B* **41** (2010) 295
2. O. V. Chemezov, O. N. Vinogradov-Jabrov, A. P. Apisarov, A. V. Isakov, S. V. Plaxin, V. B. Malkov, Yu. P. Zaikov, in *Proceedings of the Conference*, *Silicon for the Chemical and Solar Industry X*, Ålesund - Geiranger, Norway, 2010, Norwegian University of Science and Technology, Trondheim, 2010, p. 71
3. Y. Q. Lai, M. Jia, Z. L. Tian, J. Li, J. F. Yan, J. G. Yi, Z. G. Wang, Y. X. Liu, *Met. Mat. Trans., A* **41** (2010) 929
4. O. V. Chemezov, O. N. Vinogradov-Zhabrov, V. P. Batukhtin, A. P. Apisarov, A. V. Isakov, Yu. P. Zaikov, (Institute of High Temperature Electrochemistry, UB RAS), Pat. RF No 2399698 (2009)
5. O. V. Chemezov, V. P. Batukhtin, A. P. Apisarov, A. V. Isakov, Yu. P. Zaikov, (Institute of High Temperature Electrochemistry, UB RAS), Pat. RF No 2427526 (2010)
6. T. E. Schlesinger, K. Rajeshwar, N. R. De Tacconi, *Electrodeposition of semiconductors*, in *Modern Electroplating*, M. Schlesinger, M. Paunovic, Eds., Wiley, New York, 2001, p. 383
7. D. B. Frolenko, Z. S. Martem'yanova, A. N. Baraboshkin, S. V. Plaksin, *Rasplavy* **5** (1993) 42
8. D. B. Frolenko, Z. S. Martem'yanova, Z. I. Valeev, A. N. Baraboshkin, *Electrokhim.* **28** (1992) 1737
9. V. A. Isaev, *Electrochemical phase formation*, UB RAS, Ekaterinburg, 2007
10. Yu. P. Zaykov, S. I. Zhuk, A. V. Isakov, O. V. Grishenkova, V. A. Isaev, *J. Solid State Electrochem.* **19** (2015) 1341
11. A. L. Bieber, L. Massot, M. Gibilaro, L. Cassayre, P. Chamelot, P. Taxil, *Electrochim. Acta* **56** (2011) 5022
12. A. L. Bieber, L. Massot, M. Gibilaro, L. Cassayre, P. Taxil, P. Chamelot, *Electrochim. Acta* **62** (2012) 282
13. S. V. Kuznetsova, V. S. Dolmatov, S. A. Kuznetsov, *Russ. J. Electrochem.* **45** (2009) 742
14. J. De Lepinay, J. Bouteillon, S. Traore, D. Renaud, M. J. Barbier, *J. Appl. Electrochem.* **17** (1987) 294
15. R. Boen, J. Bouteillon, *J. Appl. Electrochem.* **13** (1983) 277
16. D. Elwell, G. M. Rao, *Electrochim. Acta* **27** (1982) 673
17. Yu. K. Delimarskii, N. N. Storchak, R. V. Chernov, *Electrokhim.* **9** (1973) 1443
18. K. Maeda, K. Yasuda, T. Nohira, R. Hagiwara, T. Homma, *J. Electrochem. Soc.* **162** (2015) D444
19. K. Maeda, K. Yasuda, T. Nohira, R. Hagiwara, T. Homma, *ECS Trans.* **64** (2014) 285
20. O. I. Boiko, Yu. K. Delimarskii, R. V. Chernov, *Ukr. Khim. Zhurn.* **51** (1985) 385
21. Yu. P. Zaikov, A. A. Redkin, A. P. Apisarov, I. V. Korzun, N. P. Kulik, A. V. Isakov, A. A. Kataev, O. V. Chemezov, *J. Chem. Eng. Data* **58** (2013) 932

22. Yu. P. Zaykov, A. V. Isakov, I. D. Zakiryanova, O. G. Reznitskikh, O. V. Chemezov, A. A. Redkin, *J. Phys. Chem., B* **118** (2014) 1584

23. Yu. P. Zaykov, A. V. Isakov, A. P. Apisarov, O. V. Chemezov, *Non-Ferrous Met.* **1** (2014) 33

24. A. A. Andriiko, E. V. Panov, O. I. Boiko, B. V. Yakovlev, O. Ya. Borovik, *Russ. J. Electrochem*. **33** (1997) 1343

25. Z. Galus, *Teoreticheskie osnovy elektrokhimicheskogo analiza*, Mir, Moskva, 1974, p. 212

26. T. Berzins, P. Delahay, *J. Am. Chem. Soc*. **75** (1953) 555

27. G. Mamantov, D. L. Manning, J. M. Dale, *J. Electroanal. Chem.* **9** (1965) 253.